Earth and Planetary Science Letters 419 (2015) 211–221

Contents lists available at ScienceDirect

Earth and Planetary Science Letters

www.elsevier.com/locate/epsl

Neodymium isotopic characterization of Ross Sea Bottom Water and its advection through the southern South Pacific

Chandranath Basak [a,*,1], Katharina Pahnke [a], Martin Frank [b], Frank Lamy [c], Rainer Gersonde [c]

[a] Max Planck Research Group for Marine Isotope Geochemistry, Institute for Chemistry and Biology of the Marine Environment (ICBM), University of Oldenburg, Carl-von-Ossietzky-Str. 9–11, 26129 Oldenburg, Germany
[b] GEOMAR Helmholtz Centre for Ocean Research Kiel, Wischhofstraße 1–3, 24148 Kiel, Germany
[c] Alfred Wegener Institute, Helmholtz Centre for Polar and Marine Research, Am Alten Hafen 26, 27568 Bremerhaven, Germany

ARTICLE INFO

Article history:
Received 6 August 2014
Received in revised form 24 February 2015
Accepted 5 March 2015
Available online 1 April 2015
Editor: G.M. Henderson

Keywords:
GEOTRACES
neodymium isotopes
rare earth elements
South Pacific
Ross Sea Bottom Water

ABSTRACT

Since the inception of the international GEOTRACES program, studies investigating the distribution of trace elements and their isotopes in the global ocean have significantly increased. In spite of this large-scale effort, the distribution of neodymium isotopes ($^{143}Nd/^{144}Nd$, ε_{Nd}) and concentrations ([Nd]) in the high latitude South Pacific is still understudied, specifically north of the Antarctic Polar Front (APF). Here we report dissolved Nd isotopes and concentrations from 11 vertical water column profiles from the South Pacific between South America and New Zealand and across the Antarctic frontal system. Results confirm that Ross Sea Bottom Water (RSBW) is represented by an ε_{Nd} value of ~ -7, and for the first time show that these Nd characteristics can be traced into the Southeast Pacific until progressive mixing with ambient Lower Circumpolar Deep Water (LCDW) dilutes this signal north of the APF. That is, ε_{Nd} behaves conservatively in RSBW, opening a path for studies of past RSBW behavior.

Neodymium concentrations show low surface concentrations and a linear increase with depth north of the APF. South of the APF, surface [Nd] is high and increases with depth but remains almost constant below ~1000 m. This vertical and spatial [Nd] pattern follows the southward shoaling density surfaces of the Southern Ocean and hence suggests supply of Nd to the upper ocean through upwelling of Nd-rich deep water. Low particle abundance due to reduced opal production and seasonal sea ice cover likely contributes to the maintenance of the high upper ocean [Nd] south of the APF. This suggests a dominant lateral transport component on [Nd] and a reduced vertical control on Nd concentrations in the South Pacific south of the APF.

1. Introduction

Preferential retention of Sm vs. Nd within the mantle creates different initial Sm/Nd ratios between mantle derived rocks and continental crustal material. Since ^{147}Sm decays to produce ^{143}Nd (at a very slow rate), rocks with different petrogenetic history develop characteristic $^{143}Nd/^{144}Nd$ ratios ($^{143}Nd/^{144}Nd$ expressed as $\varepsilon_{Nd} = [(^{143}Nd/^{144}Nd)_{measured}/(^{143}Nd/^{144}Nd)_{CHUR}] - 1 * 10^4$; CHUR = Chondritic Uniform Reservoir with $^{143}Nd/^{144}Nd = 0.512638$, Jacobsen and Wasserburg, 1980). The heterogeneous $^{143}Nd/^{144}Nd$ distribution in rocks reaches the oceans via mechanical and chemical weathering of continental rocks and subsequent transport of the particulate and dissolved material by rivers, chemical exchange between continental margins and seawater (i.e., boundary exchange), and dust input (Frank, 2002; Goldstein and Hemming, 2003; Lacan and Jeandel, 2001, 2005; Rickli et al., 2009). Once a water mass is tagged with the characteristic ε_{Nd} signatures of its formation region, Nd isotopes can be used as a water mass tracer due to the intermediate average residence time of Nd between 300 and 1000 years in the ocean (Tachikawa et al., 2003; Arsouze et al., 2009; Rempfer et al., 2011), which is shorter than the whole ocean mixing time of ~1500 years (Broecker and Peng, 1982). While Nd isotopes are considered a quasi-conservative water mass tracer in the open ocean, water masses close to continental margins can be overprinted by interactions between seawater and continental sediments, either through partial dissolution of particles or a mechanism known as 'boundary exchange' (Lacan and Jeandel, 2001, 2005).

* Corresponding author. Tel.: +1 845 365 8647.
E-mail address: cbasak@ldeo.columbia.edu (C. Basak).
[1] Now at Lamont–Doherty Earth Observatory of Columbia University, Palisades, NY 10964, USA.

http://dx.doi.org/10.1016/j.epsl.2015.03.011
0012-821X/

In the modern ocean, North Atlantic Deep Water (NADW, $\varepsilon_{Nd} = -13.5$; Piepgras and Wasserburg, 1987) and North Pacific Deep Water (NPDW, $\varepsilon_{Nd} = -4$ to -6; Piepgras and Jacobsen, 1988; Amakawa et al., 2009) represent the two major deep water ε_{Nd} endmembers, which is a consequence of weathering inputs from older cratonic rocks in the North Atlantic and young volcanic rocks in the North Pacific. Simple mixing of these waters in the Southern Ocean are thought to dominantly determine the isotopic composition of Circumpolar Deep Water (CDW) with an intermediate ε_{Nd} value of -8 to -9 (Goldstein and Hemming, 2003; Stichel et al., 2012; Garcia-Solsona et al., 2014) but weathering contributions from Antarctica to the Southern Ocean ε_{Nd} have also recently been reported to play some role (Carter et al., 2012; Stichel et al., 2012; Rickli et al., 2014). In contrast to the Nd isotope distributions in the ocean, which appear to be dominated by advection and mixing of water masses, Nd concentrations generally show a nutrient-like behavior with increasing [Nd] with water depth, indicating a dominant vertical control (Elderfield and Greaves, 1982).

The circulation of the Southern Ocean is dominated by the westerly wind driven eastward moving Antarctic Circumpolar Current (ACC), which reaches abyssal depths and connects all major ocean basins (Talley et al., 2011 and references therein). The Southern Ocean is further characterized by the circum-Antarctic frontal system, which consists of the upward shoaling of density surfaces towards the south that create bands of steep meridional hydrographic gradients at the surface (Nowlin et al., 1977; Orsi et al., 1999). The South Pacific, which represents the largest sector of the Southern Ocean, hosts areas of major intermediate and bottom water formation (Tsuchiya and Talley, 1996; Orsi and Wiederwohl, 2009), thus making it a key area for better understanding present and past deep ocean circulation. The latitudinal location of the Pacific Subantarctic Front (SAF) reaches its southernmost position in the eastern South Pacific (Orsi et al., 1995; Talley et al., 2011). South of the SAF, the APF is represented by a strong eastward flow and upwelling of deep waters south of it. Similar to the rest of the Southern Ocean, these frontal systems in the South Pacific are associated with steep meridional gradients in surface hydrographic properties and upwelling of deep waters south of the APF. Very little is known about the behavior of dissolved Nd isotopes and concentrations in the South Pacific and their distribution in relation to the Antarctic fronts.

Over the last few years, the international GEOTRACES program has generated high-resolution data for many ocean basins to improve our understanding of the "biogeochemical cycles and large-scale distributions of trace elements and their isotopes in the marine environment" (Henderson et al., 2007). Only a limited number of dissolved Nd isotope data is available from the South Pacific sector of the Southern Ocean; these are located around the southern boundary of the ACC and one station immediately north of the APF (Carter et al., 2012; Rickli et al., 2014), leaving data gaps across the high latitude South Pacific that have so far prevented a comprehensive understanding of the ε_{Nd} and [Nd] behavior in this region. Carter et al. (2012) reported that Nd isotopes in the middle of the water column behave conservatively at open ocean stations. Closer to the Antarctic continent, CDW signatures are modified to more radiogenic values due to exchange with the margins (Carter et al., 2012). The same mechanism was inferred for the isotopic signature of Antarctic Bottom Water (AABW) formed in the Ross Sea (Rickli et al., 2014). At depth, AABW actively forms along the Antarctic shelf in the Weddell Sea, Ross Sea, Adélie Coast, and Prydz Bay (Orsi et al., 1999). Continental Antarctica consists of diverse types of bedrock of different ages with a wide range of ε_{Nd} values (Roy et al., 2007), which can be hypothesized to tag the deep water formed in different regions with different ε_{Nd} signatures. The study presented here adds new dissolved Nd isotope data to test whether the RSBW ε_{Nd} signature in the Ross Sea can be traced along the flow path of RSBW into the Southeast Pacific.

Here we report dissolved Nd isotope and Nd concentrations from 11 vertical profiles from across the South Pacific between South America and New Zealand and between 46° S and 69° S (Fig. 1). The samples cover different water masses (Fig. 2) east and west of the Pacific-Antarctic Ridge and across the circum-Antarctic fronts, allowing insight into mixing processes of different water masses and their origins. The [Nd] distribution across the circum-Antarctic frontal system is interpreted in the context of deep-water upwelling and productivity. The Nd isotope distribution enables the tracing of AABW formed in the Ross Sea into the Southeast Pacific.

2. General hydrography

Volumetrically speaking, the most important water mass of the deep ACC is CDW. Deep waters of North Atlantic (NADW), North Pacific (NPDW), and Indian Ocean (Indian Ocean Deep Water (IDW)) origin enter the Southern Ocean and mix to form the main body of the CDW (Talley et al., 2011). It can be subdivided into the oxygen-depleted and nutrient-rich Upper CDW (UCDW) and the more saline Lower CDW (LCDW) (Reid and Lynn, 1971; Orsi et al., 1995; Talley et al., 2011). The UCDW, which acquires its oxygen minimum from IDW and NPDW, is defined by a density range of 27.55 kg/m^3 $< \gamma^n <$ 28 kg/m^3. The oxygen minimum of UCDW is most prominent at 1500 m water depth immediately north of the SAF (Talley et al., 2011). The LCDW is defined by a neutral density range of 28.00 kg/m^3 $< \gamma^n <$ 28.27 kg/m^3 and a salinity maximum that is inherited from NADW (Reid and Lynn, 1971; Reid, 1994; Orsi et al., 1995; Whitworth et al., 1998). Lower CDW occupies the deep South Pacific north of the SAF and progressively shoals to 700–400 m water depth in the Antarctic Zone (AZ) south of the APF (Talley et al., 2011). At several locations, the upwelled LCDW reaches Antarctic continental shelves, mixes with dense shelf waters and sinks to the abyss, forming AABW (Foster and Carmack, 1976; Jacobs et al., 1970; Orsi et al., 1999). North of the SAF, Antarctic Intermediate Water (AAIW; 27.13 kg/m^3 $< \gamma^n <$ 27.55 kg/m^3) found between 500–1500 m water depth within the eastern South Pacific is characterized by low salinity and a high oxygen content (Talley, 1996; Whitworth and Nowlin, 1987). North Pacific Deep Water (NPDW), unlike NADW, is composed of recycled deep water from the Southern Hemisphere. The NPDW flows south at 1500–3500 m water depth as a low-oxygen water mass and enters the South Pacific between the East Pacific Rise and South America (Kawabe and Fujio, 2010; Molina-Kescher et al., 2014).

The Ross Sea is one of the major sites of AABW formation (Orsi and Wiederwohl, 2009). Sea-ice production and associated brine rejection transforms the near freezing Antarctic Surface Water into dense Shelf Water, which continuously interacts with the overlying modified CDW to produce dense transitional waters known as Modified Shelf Water (MSW). Once this highly dense MSW has sunk into the adjacent Antarctic basins, it is generally recognized as AABW (Orsi et al., 1999; Orsi and Wiederwohl, 2009). The AABW formed in the Ross Sea (Ross Sea Bottom Water, RSBW) is the coldest ($-0.3°$ to 0 °C) and saltiest (34.7–34.72) bottom water in the Southern Ocean with a neutral density >28.27 kg/m^3 (Jacobs et al., 1970; Orsi and Wiederwohl, 2009). Through mixing with overlying LCDW, the hydrographic properties of AABW are quickly eroded along its northward flow path.

3. Materials and methods

South Pacific seawater samples were collected during expedition ANT-XXVI/2 (November 2009–January, 2010) aboard *F/S Po-*

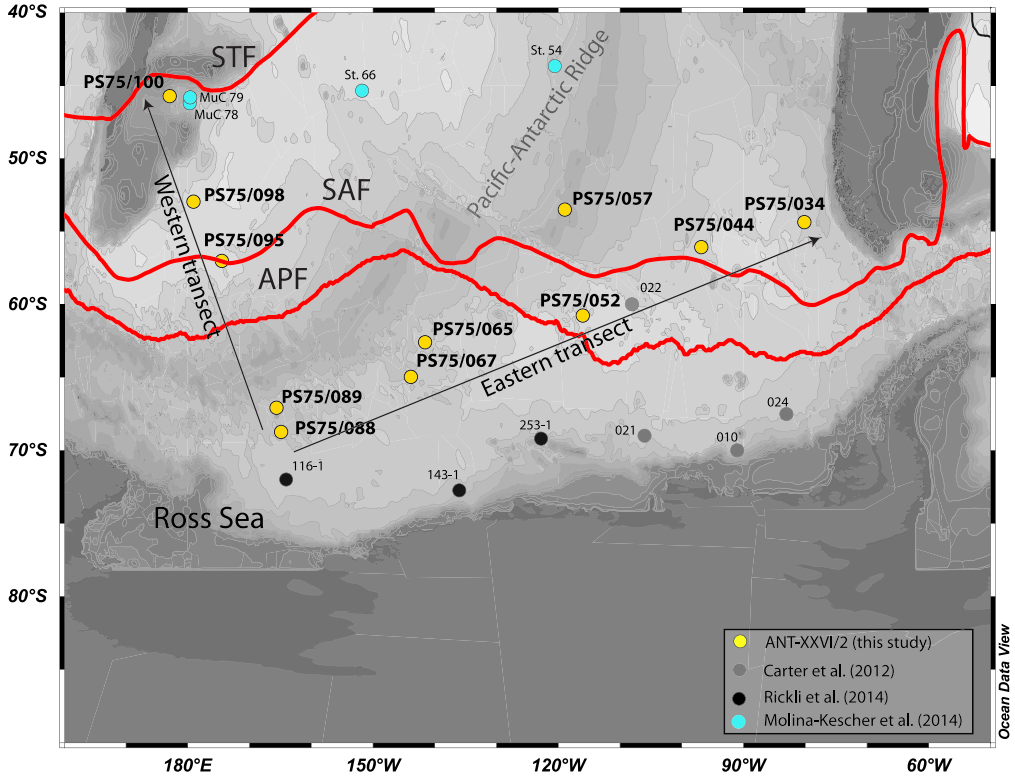

Fig. 1. Station map of samples collected during *F/S Polarstern* expedition ANT-XXVI/2. The stations are divided into an eastern and western transect. Light grey, black, and cyan colored symbols represent the stations from Carter et al. (2012), Rickli et al. (2014), and Molina-Kescher et al. (2014) respectively. STF = Subtropical Front; SAF = Subantarctic Front; APF = Antarctic Polar Front (frontal locations after Orsi et al., 1995). (For interpretation of the references to color in this figure legend, the reader is referred to the web version of this article.)

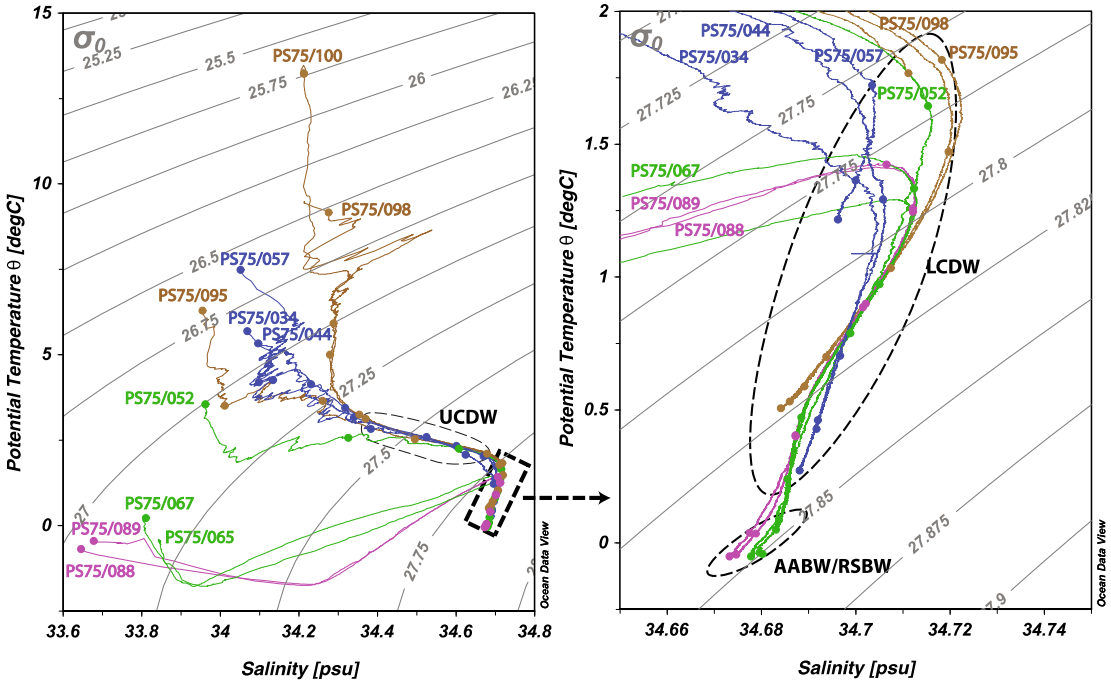

Fig. 2. Potential temperature (θ)–salinity diagram showing all studied stations. (a) Full potential temperature-salinity range. (b) Detailed diagram of all deep samples. Marked water masses are based on neutral density values (Whitworth et al., 1998). UCDW = Upper Circumpolar Deep Water; LCDW = Lower Circumpolar Deep Water; AABW = Antarctic Bottom Water; RSBW = Ross Sea Bottom Water. Along the eastern transect, blue and green colors represent stations north and south of SAF respectively. Brown and pink colors represent stations north and south of the SAF, respectively, along the western transect. (For interpretation of the references to color in this figure legend the reader is referred to the online version of this article.)

larstern for dissolved neodymium isotope composition and concentration ([Nd]) measurements. The cruise track from Punta Arenas (Chile) to Wellington (New Zealand) covered the subantarctic to polar South Pacific allowing sample collection at 11 stations across all frontal systems (Fig. 1; Table S1). All samples were collected from 12 L standard Niskin bottles (Ocean Test Equipment Inc.) mounted on a CTD rosette. Approximately 7–10 L of seawater per sample were filtered directly from the Niskin bottles into pre-cleaned collapsible 10 L LDPE containers for Nd isotopes, and into pre-cleaned 0.5 L LDPE bottles for [Nd] measurements using AcroPak500 filter cartridges (0.8/0.45 μm pore size). Each filter was dedicated to a specific depth range and was used for that depth range at each station. Filters were pre-cleaned with 1N HCl and rinsed with MilliQ water, followed by flushing with seawater prior to first use. The same sampling procedure was used on the US GEOTRACES North Atlantic cruise (GA03) and intercalibration at crossover stations shows that carry-over from the previous station does not pose a problem with the measured seawater Nd isotope values or concentrations (see Stichel et al., 2015). Following filtration, the water samples were acidified with quartz-distilled 6N hydrochloric acid (HCl) to a target pH of 3.5 for Nd isotopes and a pH of $\leq$2 for [Nd] analyses. Samples collected for [Nd] measurements were stored for onshore treatments. Samples for Nd isotopes were pre-concentrated onboard using C_{18} SepPak® cartridges (Waters Inc.; 1 cartridge per 5L seawater) pre-loaded with an REE complexing agent (HDEHP) (modified after Jeandel et al., 1998 and references therein). The C_{18} cartridges were then wrapped in Parafilm® and stored for further treatment in the shore-based laboratory. To avoid shipboard contamination, the entire process of acidification and pre-concentration of seawater was carried out under a temporary 'clean-bubble' (using plastic sheets) in one of the wet labs on *R/V Polarstern*.

Once back in the home laboratory, samples for dissolved Nd isotopes and concentrations were processed using different chromatographic procedures. Detailed chemical separation and mass spectrometric methodologies are described in the online Supplementary Material (SOM). Six full water column seawater Nd isotope profiles were measured using a ThermoScientific *Neptune Plus* multi-collector inductively coupled plasma mass-spectrometer (MC-ICP-MS) at the University of Oldenburg, and three profiles were analyzed at GEOMAR, Kiel, on a Nu Instruments MC-ICP-MS. Samples from two remaining profiles were analyzed at the University of Hawaii using a VG Sector thermal ionization mass spectrometer (TIMS). All dissolved Nd concentration measurements were done by isotope dilution at the University of Oldenburg.

For samples analyzed at the University of Oldenburg, typical long-term external errors (reported as 2σ SD, Table S1 of the SOM) range between 0.2 and 0.3ε_{Nd}, based on multiple JNdi-1 analyses during each session. The errors on [Nd] concentration measurements are typically below 5% with a few exceptions of 10–18% (see Table S1). A combined cruise, chemistry, and analytical blank was measured to be ~200 pg Nd for the Nd isotopes procedure (~3% of the lowest sample concentration measured) and ~1 pg for [Nd] analyses, and hence considered negligible. The errors on isotope measurements carried out at GEOMAR, Kiel, and the University of Hawaii are described in detail in Molina-Kescher et al. (2014) and Pahnke et al. (2012), respectively. Geomar and the University of Hawaii and authors C. Basak and K. Pahnke successfully participated in the GEOTRACES intercalibration (van de Flierdt et al., 2012). Analyses of the intercalibration samples at the University of Oldenburg are also well within the uncertainty of the intercalibration measurements (M. Behrens, K. Pahnke, 2013, unpubl. data).

In order to check the reliability of the data reported in this study, the vertical ε_{Nd} and [Nd] profiles from station PS75/052 are compared with the nearby open ocean station 022 (60°32 S, 108°18 W) of Carter et al. (2012) (Fig. 3a, b). Except for the surface, which is subject to seasonal and interannual variability, the ε_{Nd} data of these two stations agree within the analytical uncertainty (Fig. 3a). The Nd concentrations for the six depths that overlap in both profiles agree within 1.24 pmol/kg (Fig. 3a). A comparison between PS75/088 and the Ross Sea station 116-1 (72°37 S, 164°05 W) of Rickli et al. (2014) is within error except for the sample at 3000 m water depth and the upper 500 m for ε_{Nd} (Fig. 3c). The overall structure of the [Nd] depth profile at station PS75/088 is similar to that at station 116-1 (Rickli et al., 2014), but absolute concentrations are lower at PS75/088 located further north of 116-1. This disagreement in ε_{Nd} and [Nd] is likely due to the latitudinal offset and the diminishing influence of continental Nd input from Antarctica.

4. Results

4.1. Hydrography at the stations

The stations studied here are divided into an eastern transect, extending from north of the SAF to the Ross Sea (stations PS75/034 to PS75/088) and a western transect extending from the Ross Sea to New Zealand (stations PS75/088 to PS75/100) (Fig. 1). Stations along the eastern transect that are located north of the SAF (PS75/034, PS75/044, PS75/057) are bathed by bottom waters with a neutral density range of 28.24–28.08 kg/m^3 that is characteristic for LCDW (Orsi et al., 1995; Whitworth et al., 1998). Water at a depth of 1500 m is characterized by a potential temperature of ~2.5 °C (Fig. 2), densities of 27.76 kg/m^3 $< \gamma^n <$ 27.85 kg/m^3, and low oxygen concentrations (Fig. 4), indicating the presence of UCDW (Orsi et al., 1995; Whitworth and Nowlin, 1987). At eastern stations south of the SAF (PS75/052, PS75/065, PS75/067, PS75/088), bottom waters have $\gamma^n \geq$ 28.28 kg/m^3, characteristic of RSBW (Orsi et al., 1999; Orsi and Wiederwohl, 2009). The water mass immediately above RSBW at these stations is LCDW.

The UCDW shoals towards the south and reaches to below the surface waters in the AZ and is completely absent south of the AZ (Orsi et al., 1995; Talley et al., 2011). Station PS75/052, located within the AZ, is therefore influenced by UCDW at 500–1000 m water depth, while stations PS75/067 and PS75/088 south of the AZ lack UCDW.

Along the western transect (stations PS75/100, PS75/098, PS75/095, PS75/089, PS75/088) (Fig. 1), stations close to New Zealand and north of the SAF (PS75/100, PS75/098) exhibit an oxygen minimum at 1500–2000 m water depth that marks the presence of UCDW, while it is missing at stations at and south of the SAF (Fig. 4). Based on neutral density, the water mass below 2800 m at stations PS75/095 and PS75/098 is LCDW. Although a prominent oxygen minimum is not observed at station PS75/095, the presence of UCDW at water depths of 1000 m is evident from its characteristic potential temperature (~2.5 °C) and neutral density (γ^n = 27.75 kg/m^3). Deep water (>3000 m) at stations PS75/088 and PS75/089 is characterized by high neutral density ($\gamma^n >$ 28.27 kg/m^3), characteristic of RSBW (Orsi et al., 1999; Orsi and Wiederwohl, 2009).

4.2. Seawater Nd isotopes

For clarity, the dissolved Nd isotope data (n = 66) are reported and discussed following the division of the stations into an eastern and western transect used above (Figs. 3, 4; all data are listed in Table S1 (SOM) and on Pangaea (www.pangaea.de) under doi: 10.1594/PANGAEA.834728).

Based on hydrographic properties the deep waters (>3000 m) at stations closest to the Ross Sea (PS75/088, PS75/089) are occupied by RSBW (Fig. 2), which carries an ε_{Nd} signature at these stations of −7.5 to −7.2.

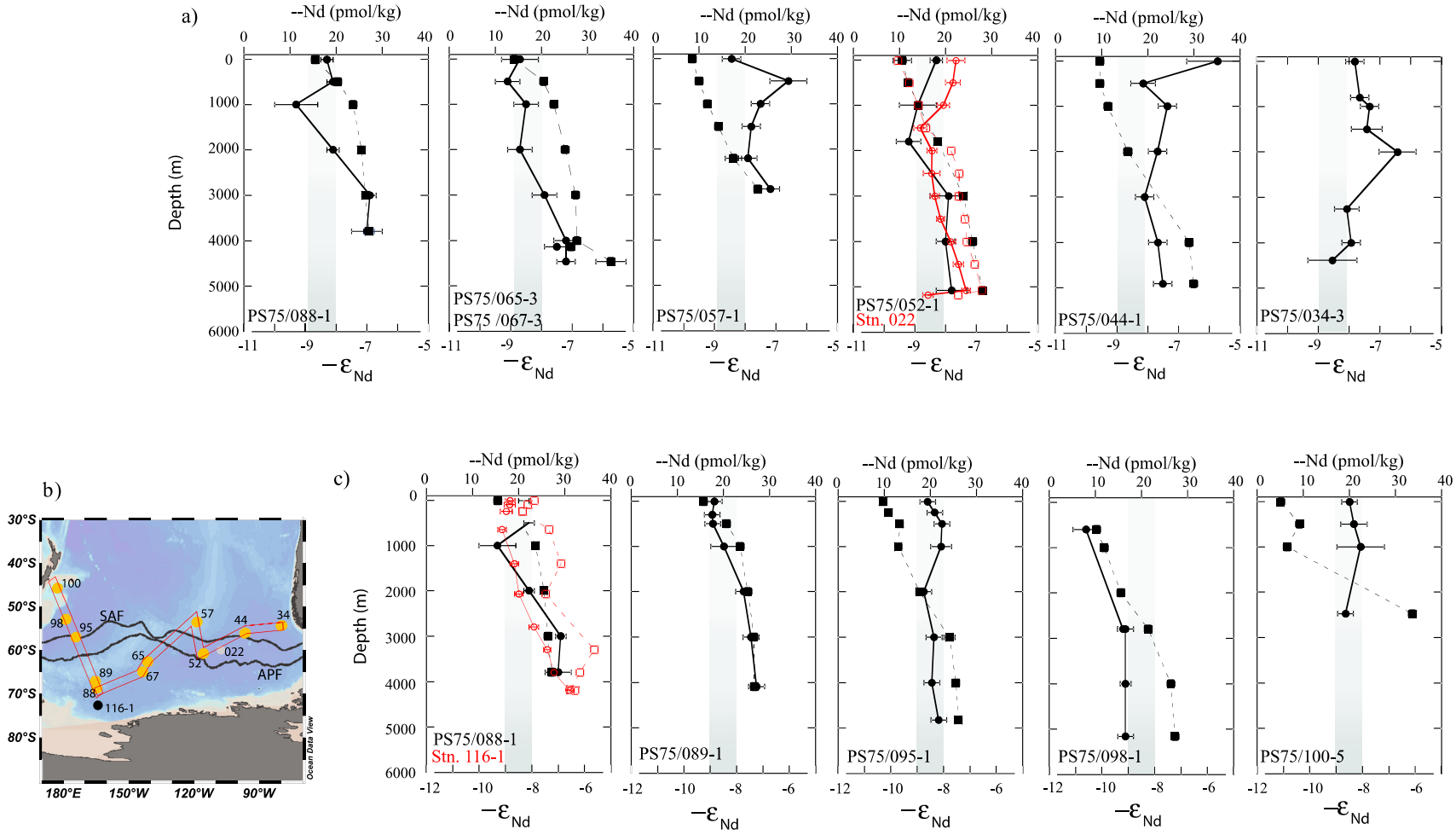

Fig. 3. Vertical profiles of Nd isotope ratios (ε_{Nd}) and Nd concentrations ([Nd]) along the eastern and western transect, ε_{Nd} (solid circles) and [Nd] (solid squares). (a) Eastern transect, (b) map showing the station locations, (c) western transect. Faded grey bar indicates the range of ε_{Nd} values typical of Circumpolar Deep Water (CDW) (Stichel et al., 2012). Red symbols plotted together with station PS75/052 and PS75/088 are ε_{Nd} (empty red circles) and [Nd] (empty red squares) from adjacent open ocean station 022 (Carter et al., 2012) and 116-1 (Rickli et al., 2014). Error bars for ε_{Nd} are typically 2σ external reproducibility of JNdi-1 analyzed during the analytical sessions. Where the internal errors are larger than external reproducibility, propagated errors are reported. Majority of reported errors for [Nd] are smaller than the symbol size. (For interpretation of the references to color in this figure legend, the reader is referred to the web version of this article.)

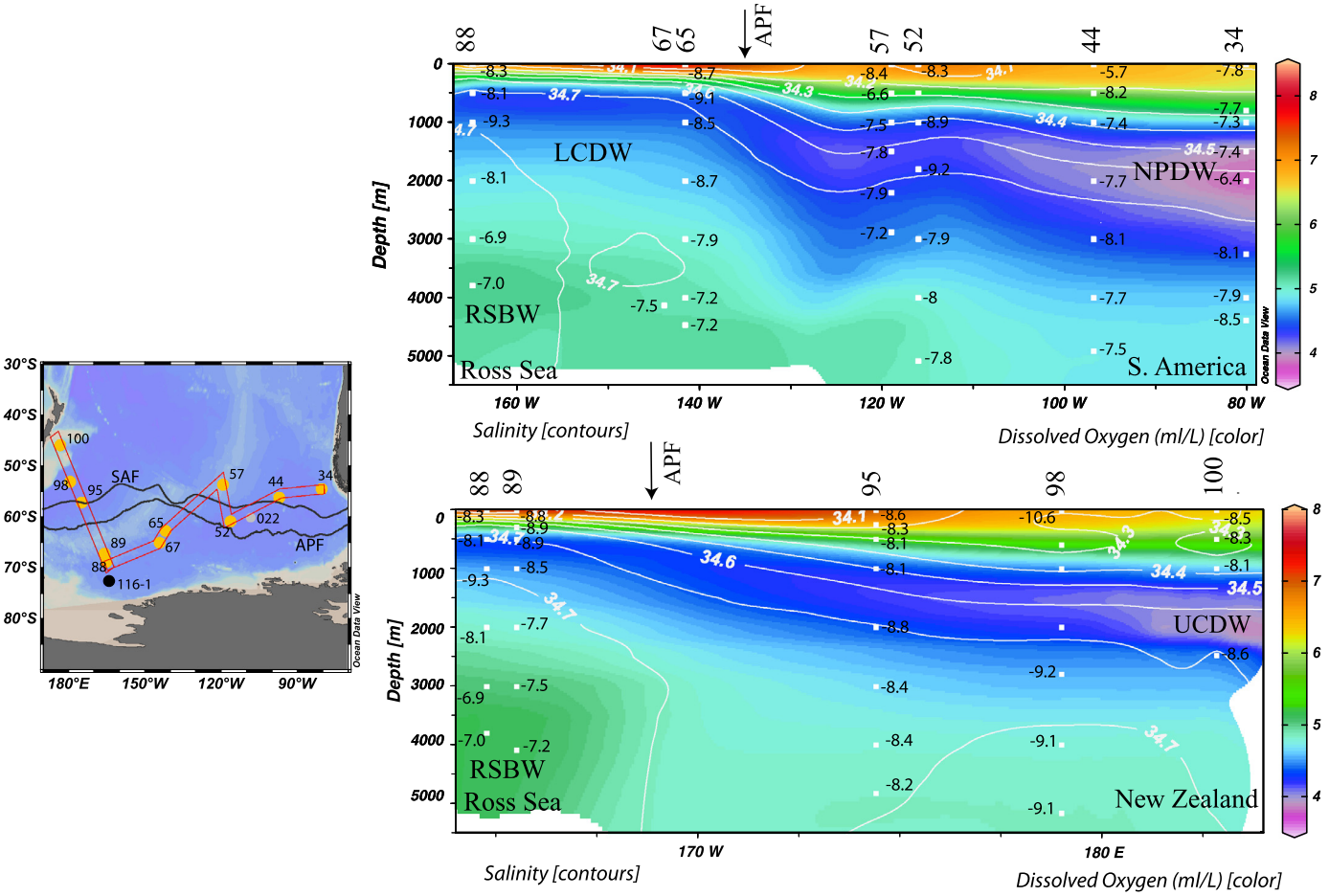

Fig. 4. Map showing the location of the stations and the section (station names abbreviated). Distribution of dissolved oxygen (Garcia et al., 2010) and salinity (Antonov et al., 2010) *vs.* depth along the eastern and the western transect are shown in the upper and lower panel, respectively. Positions of the Antarctic Polar Front (APF) and Subtropical Front (STF) after Orsi et al. (1995). CDW = Circumpolar Deep Water; UCDW = Upper Circumpolar Deep Water; RSBW = Ross Sea Bottom Water. (For interpretation of the references to color in this figure legend, the reader is referred to the web version of this article.)

Along the eastern transect, ε_{Nd} ranges from −5.7 to −9.2 (Fig. 3a; Table S1). Physical properties indicate that the predominant water mass along the eastern transect is CDW with average ε_{Nd} values of −8 to −9 (Jeandel, 1993; Stichel et al., 2012; Carter et al., 2012; Rickli et al., 2014; Garcia-Solsona et al., 2014). The presence of the radiogenic ε_{Nd} signature of RSBW can be tracked along the transect towards the northeast (PS75/065, PS75/067, PS75/052, PS75/044), where both ε_{Nd} and neutral density characteristics reflect progressive mixing of RSBW with overlying CDW (Fig. 5). At stations north of the SAF (PS75/034, PS75/044, PS75/057), waters between 1000–2000 m water depths are UCDW and exhibit an ε_{Nd} of >-8 (Figs. 3a, 4). Pure AAIW is found between 500–1000 m water depth at these stations with an ε_{Nd} of −6.6 to −8.2 (Fig. 3a; Table S1).

The ε_{Nd} values of the western transect range from −6.9 to −10.6 (Fig. 3c, Table S1). Hydrographic properties indicate the predominant presence of CDW at water depths >1000 m at the majority of the stations (PS75/095, PS75/098, PS75/100) and a corresponding ε_{Nd} of −8 to −9.

4.3. Seawater Nd concentrations

Vertical Nd concentration profiles in the South Pacific follow two general patterns depending on their position relative to the APF (Fig. 8b). North of the APF, Nd concentrations are low at the surface (∼10 pmol/kg) and increase linearly with depth, reaching bottom water values of 25–30 pmol/kg. Station PS75/100 close to

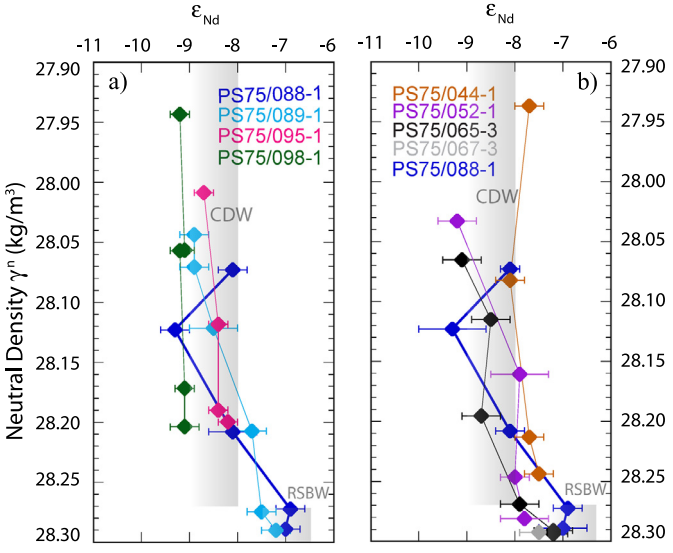

Fig. 5. ε_{Nd} *vs.* neutral density (γ^n) for deep samples. (a) Western transect. (b) Eastern transect. Only open ocean stations are considered. Near shelf stations (PS75/034, PS75/100) and the deepest sample from PS75/057 hold potential to be affected by boundary exchange and are excluded in this figure. Vertical grey bars indicate the range of RSBW and CDW. (For interpretation of the references to color in this figure legend, the reader is referred to the web version of this article.)

New Zealand exhibits the lowest upper-ocean [Nd] (5–10 pmol/kg, 11–1000 m water depth) and an anomalously high bottom water [Nd] (33.7 pmol/kg at 2475 m water depth). South of the APF, surface concentrations are higher (~15 pmol/kg) than north of the APF, increase towards 1000 m water depth, and are almost constant between 1000 m and the bottom (~25–30 pmol/kg). Station PS75/065 shows an elevated bottom water [Nd] (35.1 pmol/kg).

5. Discussion

5.1. Distribution of ε_{Nd}

5.1.1. Eastern transect

The bottom water at station PS75/088 closest to the Ross Sea is clearly identifiable as RSBW based on its neutral density and is represented by an average ε_{Nd} signature of -7 ± 0.5 (Figs. 2, 3, Table S1 SOM). This ε_{Nd} value is the most radiogenic of all deep and bottom water values of our stations and also much more radiogenic than all reported ε_{Nd} values for AABW in the South Atlantic ($\varepsilon_{Nd} = -8.5$ to -10.8; Stichel et al., 2012; Garcia-Solsona et al., 2014). A similar bottom water ε_{Nd} value of ~ -7 has been reported by Rickli et al. (2014) from a station south of PS75/088 (Fig. 1), emphasizing the characteristic Nd isotopic value of bottom water forming in the Ross Sea. We suggest that modified shelf water in the Ross Sea acquires this signature from the Ross Sea shelf before it spills over the shelf edge into the abyssal basin to form RSBW. The Nd isotopic composition of the lithogenic <63 μm core top sediment fraction from areas surrounding the Ross Sea ranges between $\varepsilon_{Nd} = -6.7$ and -7.3 (Roy et al., 2007), while late Quaternary tills (<63 μm) show a range of -5.8 to -7.5 and -3.8 to -6.9 for the western and eastern Ross Sea, respectively (Lang-Farmer et al., 2006). These terrigenous values represent the average ε_{Nd} of nearshore sources and support the hypothesis that AABW formed in the Ross Sea acquires its ε_{Nd} signature of ~ -7 from Ross Sea shelf sediments. The observed bottom water radiogenic ε_{Nd} signature can be clearly traced into the Southeast Pacific along our eastern transect (PS75/065, PS75/067) before it is progressively mixed with ambient LCDW, as also evident from hydrographic properties (Fig. 5). This demonstrates the conservative behavior of ε_{Nd} in RSBW and its potential to trace RSBW along its flow path, hence also enabling its use for paleoceanographic studies.

The bottom water at site PS75/052 (5083 m; $\varepsilon_{Nd} = -7.8 \pm 0.5$) is hydrographically comparable to the two deepest samples at nearby station 022 of Carter et al. (2012), for which ε_{Nd} values of -7.3 ± 0.1 (5081 m) and -8.6 ± 0.2 (5182 m) were reported (Figs. 1, 3). Carter et al. (2012) explained the lower ε_{Nd} of the deepest sample (8 m above the seafloor) through a local overprint from bottom sediments. Overprints from bottom sediments are not observed in any of the bottom samples in this study (except for station PS75/057 on the Pacific–Antarctic Ridge, see below), most likely due to the greater distance of the deepest samples from the seafloor (14–101 m).

At station PS75/044, neutral density values indicate that the bottom, deep and mid-depth waters are represented by LCDW and UCDW, respectively. The corresponding ε_{Nd} values range from -7.5 ± 0.3 to -8.1 ± 0.2, with the deepest sample exhibiting residual influence of RSBW. The bottom to mid-depth waters at site PS75/034 are outside the range of RSBW densities and exhibit ε_{Nd} values similar to CDW ($\varepsilon_{Nd} = -7.9 \pm 0.3$ to -8.5 ± 0.7). Thus, a distinction between UCDW and LCDW cannot be clearly made based on the ε_{Nd} signature at these two eastern transect stations. Stichel et al. (2012) also reported no distinction between upper and lower CDW in the South Atlantic based on ε_{Nd} values. Station PS75/057 is located on the Pacific–Antarctic Ridge and is the shallowest station along the eastern transect with a bottom depth of 2878 m and an ε_{Nd} value of -7.2 ± 0.3 in the deepest sample (Fig. 3). According to the θ–S properties and neutral density, the bottom water at this site is LCDW (Figs. 2, Table S1), which at other stations and in the South Atlantic carries an isotope signature of $\varepsilon_{Nd} = \sim -8$ to -9 (Stichel et al., 2012). The station is located above the ridge flank and we therefore suggest that the radiogenic bottom water ε_{Nd} at this site is caused by boundary exchange with the basaltic rocks of the ridge (Lacan and Jeandel, 2005; Rickli et al., 2010; Pearce et al., 2013).

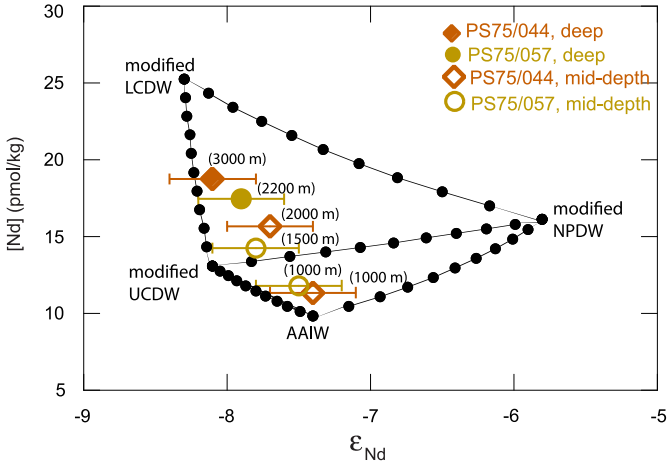

Fig. 6. Simple mixing model using three predominant South Pacific water masses as endmembers. All endmember values were chosen to represent the respective water masses close to our study area (not at their site of formation). Details of individual endmembers used are provided in the SOM. The solid black circles along the mixing lines are 10% mixing increments. (For interpretation of the references to color in this figure legend, the reader is referred to the web version of this article.)

Intermediate to shallow water depths at the stations north of the SAF along the eastern transect (PS75/034, PS75/044, PS75/057) carry an ε_{Nd} value of ~ -8. The isotopic composition is shifted to significantly more radiogenic values ($\varepsilon_{Nd} = -6.4 \pm 0.5$ to -7.7 ± 0.3) at ~1000–2000 m water depth. North Pacific Deep Water is characterized by low oxygen concentrations and radiogenic Nd isotope values (ε_{Nd} -5.8 to > -4) in the North Pacific and along its flow path (Grasse et al., 2012; Molina-Kescher et al., 2014), and flows southward in the East Pacific (Talley et al., 2011; Kawabe and Fujio, 2010). Contributions from NPDW to the waters north of the SAF can thus explain the observed shift towards more radiogenic seawater ε_{Nd}. In order to test this, we compare our deep water compositions in a water mass mixing diagram assuming conservative mixing between NPDW, UCDW, LCDW, and AAIW (Fig. 6). For Nd concentrations, we use modified endmember values that are directly relevant to our study area, that is, we take into account the observed decrease in [Nd] across the APF at UCDW and LCDW depth (Fig. 6), and the pronounced removal of Nd from NPDW in the high productivity area of the Eastern Equatorial Pacific (EEP) (Grasse et al., 2012; Molina-Kescher et al., 2014). All data from 1500–3000 m water depth and north of the SAF (PS75/044, PS75/057) are within the mixing envelopes defined by modified UCDW, LCDW, and NPDW (Fig. 6). Supported by the neutral density, a dominant UCDW influence is observed in the shallower samples (~1000–2000 m) that also show the highest NPDW contribution of 10–15% (Fig. 6). Station PS75/034 lacks Nd concentration data and is therefore not included in Fig. 6. However, the ε_{Nd} of -6.4 at 2000 m water depth at this station suggests higher NPDW influence than at stations PS75/044 and PS75/057, consistent with the depth range and flow path of NPDW (Kawabe and Fujio, 2010) and the low oxygen content of the water mass at this station (Garcia et al., 2010). A higher LCDW and slightly lower NPDW influence is observed in the deeper samples (>2000 m) (Fig. 6). According to hydrographic

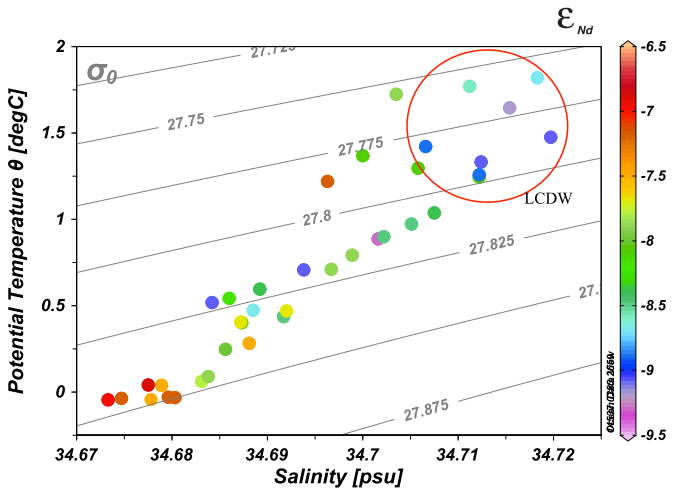

Fig. 7. Potential temperature (θ)–salinity diagram for bottom waters with a potential density >27.75 kg/m^3. Colors are ε_{Nd} values. Samples from the salinity maximum of LCDW exhibit a shift towards negative ε_{Nd}. (For interpretation of the references to color in this figure legend, the reader is referred to the web version of this article.)

properties samples at 1000 m water depth at stations PS75/044 and PS75/057 are within the transition of UCDW and overlying AAIW. Based on the mixing diagram, a mixture of ~20% modified UCDW, ~10% modified NPDW and ~70% pure AAIW best explains the Nd composition from 1000 m water depth at both stations. The anomalous value of −5.5 at the surface of station PS75/044 may be best explained as aeolian input or advected surface waters that are influenced by isotope signals from the South American shelf.

The mixing diagram therefore supports an increased contribution of NPDW to the deep waters at stations north of the SAF and hence explains the more radiogenic ε_{Nd} at those depths and locations.

5.1.2. Western transect

The ε_{Nd} distribution along the western transect is dominated by ε_{Nd} values of −8 to −9, consistent with the dominance of CDW (Fig. 3). The only more radiogenic values are observed within RSBW at stations PS75/088 and PS75/089 (see Section 5.1.1, Fig. 3). According to neutral densities, deep waters below ~2000 m along the western transect at and north of the SAF are represented by LCDW (Fig. 2), consistent with physical oceanographic studies that identified the predominance of LCDW within the Subantarctic Zone (SAZ) of the Pacific (Talley et al., 2011). Stations PS75/095 and PS75/098 show slightly more negative ε_{Nd} (−9 to −8) at depth than stations along the eastern transect (Fig. 3). Hydrographically, deep waters at these stations also differ from those along the eastern transect, consistent with the different bottom water sources in the western and eastern South Pacific separated by the Pacific-Antarctic Ridge. While the eastern basin receives RSBW ($\varepsilon_{Nd} = -7$) that mixes into LCDW, it is plausible that the western basin receives AABW with a less radiogenic ε_{Nd} signature mixed into LCDW from the Weddell Sea and Adélie Coast (Stichel et al., 2012; van de Flierdt et al., 2006). A slight negative shift towards $\varepsilon_{Nd} = -9$ is also observed at the depth of the salinity maximum of LCDW at all western transect stations south of the SAF (PS75/095, PS75/089, PS75/088) and also at the eastern transect stations south of the SAF (Fig. 7). The elevated salinity of LCDW originates from contributions of NADW (Talley et al., 2011), suggesting that remnants of the negative NADW ε_{Nd} signature ($\varepsilon_{Nd} = -13.5$ in the North Atlantic) are present in LCDW. Molina-Kescher et al. (2014) also suggested residual NADW influence within the deep water at stations close to New Zealand ($\varepsilon_{Nd} = -9$ to −10.3).

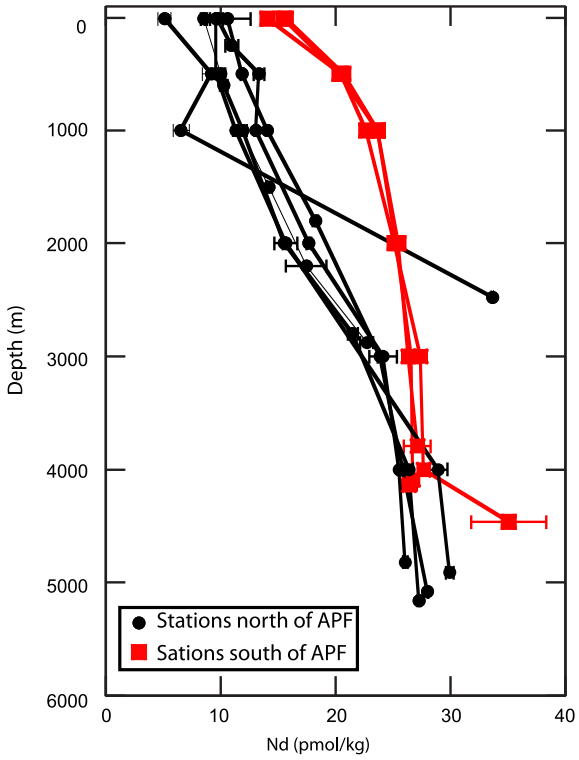

Fig. 8. Neodymium concentration profiles of all stations divided into stations located north of the Antarctic Polar Front (APF) (black circles) and south of the Polar Front (red squares). Errors associated with [Nd] measurements are reported in SOM Table S1. (For interpretation of the references to color in this figure legend, the reader is referred to the web version of this article.)

5.2. [Nd] distribution in the South Pacific

The general explanation for the nutrient-like distribution of [Nd] in the ocean is scavenging of Nd in the upper ocean through adsorption onto biogenic or lithogenic particles and release through particle decomposition at depth (Elderfield and Greaves, 1982; Siddall et al., 2008; Arsouze et al., 2009; Rempfer et al., 2011; Stichel et al., 2012). Biogenic opal production is high within and immediately north of the APF (Sigmon et al., 2002), thus abundant biogenic opal particles can explain the very low surface [Nd] at and north of the APF. South of the APF, Nd concentrations are substantially higher at the surface, increase to ~1000 m and are nearly constant from 1000 m to the bottom (Fig. 8). The [Nd] distribution closely follows the density structure of the water column, with similar [Nd] at equal neutral density and hence high [Nd] shoaling towards the south (Fig. 9). The high Nd concentrations in the upper water column and essentially constant concentrations below ~1000 m water depth at stations south of the APF therefore suggest Nd supply to the upper ocean through upwelling of deeper waters. A plot of [Nd] vs. neutral density of all samples from AAIW to AABW-depth reveals that the [Nd] of UCDW and LCDW follows linear mixing lines between AAIW and LCDW, and UCDW and AABW, respectively, suggesting a strong control of lateral transport on [Nd] in this region (Fig. 10). When compared to ideal conservative mixing as defined by the representative water mass endmembers, the [Nd] is offset to lower values in the case of UCDW and both lower and higher values in the case of LCDW, respectively (Fig. 10). This suggests Nd removal through particle flux down to UCDW depths and dominant Nd release at the depths of LCDW. Removal of dissolved Nd due to high particle fluxes at depth has been reported before from the equatorial and South Pacific (Grasse et al., 2012; Molina-Kescher et al., 2014). The deviation to higher [Nd] for

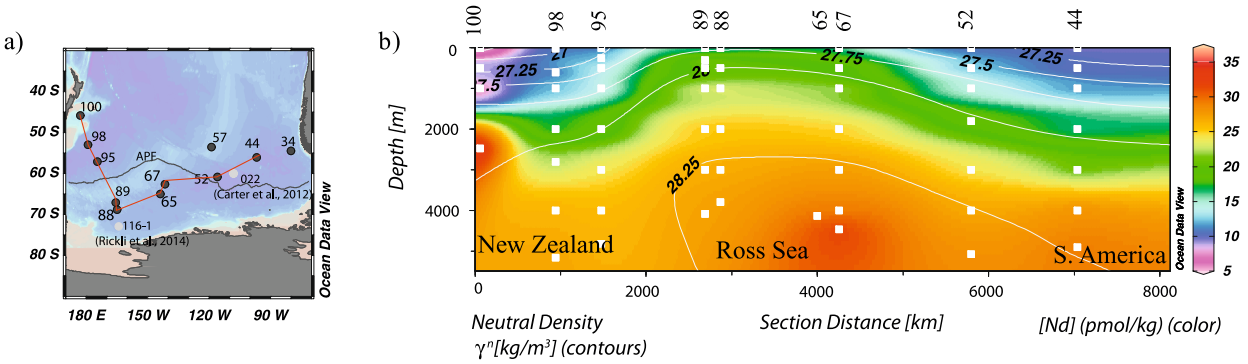

Fig. 9. Distribution of dissolved [Nd] overlain by neutral density (γ^n) contours along entire sampling track in the South Pacific. (a) Map showing the sampling locations. (b) Neutral density (γ^n) and [Nd] exhibit a tight coupling and gradually shoal towards higher latitudes (southernmost stations in the middle of the section). Sample locations are plotted as solid white sqaures. (For interpretation of the references to color in this figure legend, the reader is referred to the web version of this article.)

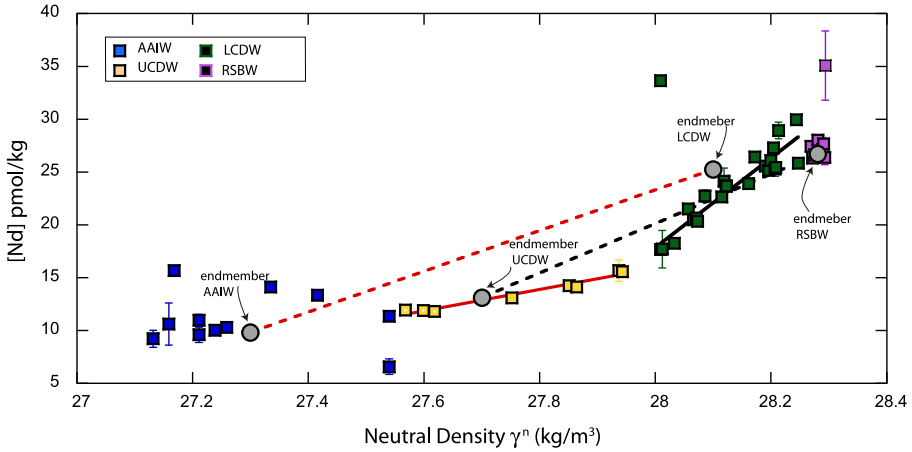

Fig. 10. Plot showing [Nd] *vs.* neutral density. Red and black solid lines represent linear regression lines through UCDW and LCDW data, respectively. One LCDW data point with high [Nd] is excluded from calculating the linear trend. Dashed lines represent the conservative mixing relationship between AAIW-LCDW, and UCDW-AABW. The endmember values are from the midpoint of the range of neutral densities for individual water masses and corresponding [Nd] from our data set (neutral density classifications of water masses are after Jacobs et al., 1970; Whitworth and Nowlin, 1987, and Whitworth et al., 1998). (For interpretation of the references to color in this figure legend, the reader is referred to the web version of this article.)

LCDW can best be explained by Nd release at depth. Thus, the [Nd] distribution in the study area is controlled by a combination of dominant lateral transport and conservative mixing, and vertical removal and release processes.

Due to the rather homogeneous ε_{Nd} distribution in upper and lower CDW, the correlation with neutral density is not as clearly seen in the ε_{Nd} distribution, except for the slightly lower ε_{Nd} associated with the salinity maximum of LCDW that shoals to the south. Upper ocean Nd supply through upwelling was recently suggested by Chen et al. (2013) based on the global relationship of [Nd] with nutrient distributions. It is clear from the above discussion that vertical cycling plays an important role in defining the [Nd] of the South Pacific sector of the Southern Ocean, however, lateral transport and conservative mixing are clearly more dominant than in other regions.

5.3. Shelf and open ocean boundary exchange

The [Nd] at station PS75/100 close to New Zealand is different from other stations reported in this study. The bottom water exhibits the highest Nd concentration (33.7 pmol/kg) among all the measured values in this study (Fig. 9). Sediment–seawater interactions, also known as boundary exchange (Jeandel et al., 2007), are described as a process of Nd isotopic modification of seawater due to isotope exchange with the sediments but without a change in dissolved Nd concentration (Lacan and Jeandel, 2001). Boundary exchange should only shift the deep water ε_{Nd} at station PS75/100 and not its [Nd], while we observe the opposite. A study in the Norwegian basin showed that simultaneous increase in bottom water [Nd] and ε_{Nd} deviations can happen due to resuspension and partial dissolution of margin sediments (Lacan and Jeandel, 2004). Support in favor of this mechanism has been recently reported by Carter et al. (2012) from shelf sites in the Amundsen and Bellingshausen Sea. At station PS75/100, a similar mechanism of resuspension and dissolution of margin sediments in this region of strong bottom currents and terrestrial input (e.g., Carter et al., 2004) can be invoked to explain the observed increase in [Nd] without any ε_{Nd} change, provided the difference between the ε_{Nd} signature of the bottom sediments and that of the overlying bottom water is very small. Sediment resuspension may also explain the observed high bottom water [Nd] at PS75/065.

Among the existing dissolved [Nd] and ε_{Nd} studies in the South Pacific (Carter et al., 2012; Molina-Kescher et al., 2014; Rickli et al., 2014), Carter et al. (2012) reported open ocean bottom water Nd concentrations (and minor changes in ε_{Nd}) which are consistently lower than the water 100 m above it, suggesting removal of Nd close to the sediment–water interface. In contrast, station PS75/052 that is closest to Carter et al.'s open ocean site 022, does not show any deviations from the vertical trend in [Nd] or ε_{Nd} in the deepest sample, which may be due to the fact that our deepest samples were collected significantly higher above the seafloor than those of Carter et al. (2012) (38 m vs. 8 m).

6. Summary and conclusions

The full water column of the remote high latitude South Pacific has been studied to better understand the behavior and distribution of dissolved Nd and its isotopic composition. The key findings of this study are:

1) Ross Sea Bottom Water is characterized by a distinct ε_{Nd} value of ~ -7 that allows differentiation of this water mass from other deep and bottom waters in the Southern Ocean, confirming the results from Rickli et al. (2014). For the first time, we show that this signature can be traced, along with the hydrographic properties of RSBW, into the eastern South Pacific until its characteristic ε_{Nd} signature is lost through mixing with ambient LCDW. Robust ε_{Nd} characterization of RSBW as an important and distinct bottom water mass in the Southern Ocean will be important for paleo-circulation studies based on ε_{Nd} in the South Pacific.

2) A shift to unradiogenic ε_{Nd} at 2000 m water depth at stations north of the SAF in the Southeast Pacific is explained by NPDW admixture of up to 10–15%. This observation is consistent with the southward flow path of NPDW into the eastern South Pacific.

3) The majority of our vertical profiles exhibit a slight negative shift towards $\varepsilon_{Nd} = \sim -9$ at the depth of the salinity maximum of LCDW. The salinity maximum represents the remnant of unradiogenic NADW within LCDW. This finding is in agreement with dissolved Nd isotope data in the southwest Pacific from Molina-Kescher et al. (2014).

4) Neodymium concentrations show a clear correspondence with the density structure of the South Pacific, with high surface and nearly constant subsurface to bottom water concentrations south of the Antarctic Polar Front, and low surface concentrations and a linear increase with depth north of the APF. This pattern suggests a dominant control of lateral transport and mixing on [Nd] in this region, and supports the supply of Nd through upwelling of deep water south of the APF, as suggested previously based on global [Nd] distributions (Chen et al., 2013).

Acknowledgements

We thank the entire scientific party, and captain and crew of R/V Polarstern expedition ANT-XXVI/2. We acknowledge the German Ministry of Education and Research for financially supporting the research cruise. We are grateful to Mario Molina-Kescher of GEOMAR for his assistance during Nd isotope analyses at GEOMAR facility. We are very thankful for all the support from the members of the MPI-Marine Isotope Geochemistry Group at the University of Oldenburg and would like to specifically mention M. Schulz and P. Böning for their help with smooth running of day to day lab activity and the multi-collector mass spectrometer. Comments from Jörg Rickli, three anonymous reviewers, and editor Gideon Henderson improved the quality of the manuscript. Funding for this project comes from the Max Planck Society and the US National Science Foundation (NSF) grant OCE07-26575 to K.P.

Appendix A. Supplementary material

Supplementary material related to this article can be found online at http://dx.doi.org/10.1016/j.epsl.2015.03.011.

References

Amakawa, H., Sasaki, K., Ebihara, M., 2009. Nd isotopic composition in the central North Pacific. Geochim. Cosmochim. Acta 73, 4705–4719.

Antonov, J.I., Seidov, D., Boyer, T.P., Locarnini, R.A., Mishonov, A.V., Garcia, H.E., Baranova, O.K., Zweng, M.M., Johnson, D.R., 2010. World Ocean Atlas 2009, vol. 2: salinity. In: Levitus, S. (Ed.), NOAA Atlas NESDIS, vol. 69. U.S. Government Printing Office, Washington, DC, p. 184.

Arsouze, T., Dutay, J.C., Lacan, F., Jeandel, C., 2009. Reconstructing the Nd oceanic cycle using a coupled dynamical–biogeochemical model. Biogeosciences 6, 2829–2846.

Broecker, W.S., Peng, T.H., 1982. Tracers in the Sea. Lamont–Doherty Geol. Obs., Palisades, NY.

Carter, L., Carter, R.M., McCave, I.N., 2004. Evolution of the sedimentary system beneath the deep Pacific inflow off eastern New Zealand. Mar. Geol. 205, 9–27.

Carter, P., Vance, D., Hillenbrand, C.D., Smith, J.A., Shoosmith, D.R., 2012. The neodymium isotopic composition of waters masses in the eastern Pacific sector of the Southern Ocean. Geochim. Cosmochim. Acta 79, 41–59.

Chen, T.Y., Rempfer, J., Frank, M., Stumpf, R., Molina-Kescher, M., 2013. Upper ocean vertical supply: a neglected primary factor controlling the distribution of neodymium concentrations of open ocean surface waters? J. Geophys. Res., Oceans 118, 3887–3894.

Elderfield, H., Greaves, M.J., 1982. The rare-earth elements in sea-water. 296, 214–219.

Foster, T.D., Carmack, E.C., 1976. Frontal zone mixing and Antarctic Bottom water formation in the southern Weddell Sea. Deep-Sea Res. Oceanogr. Abstr. 23, 301–317.

Frank, M., 2002. Radiogenic isotopes: tracers of past Ocean circulation and erosional input. Rev. Geophys. 40, 1001. http://dx.doi.org/10.1029/2000RG000094.

Garcia, H.E., Locarnini, R.A., Boyer, T.P., Antonov, J., Baranova, O.K., Zweng, M.M., Johnson, D.R., 2010. World Ocean Atlas 2009, Volume 3: Dissolved Oxygen, Apparent Oxygen Utilization, and Oxygen Saturation. In: Levitus, S. (Ed.), NOAA Atlas NESDIS 70. U.S. Government Printing Office, Washington, DC, p. 344.

Garcia-Solsona, E., Jeandel, C., Labatut, M., Lacan, F., Vance, D., Chavagnac, V., Pradoux, C., 2014. Rare earth elements and Nd isotopes tracing water mass mixing and particle–seawater interactions in the SE Atlantic. Geochim. Cosmochim. Acta 125, 351–372.

Goldstein, S.L., Hemming, S.H., 2003. Long lived isotopic tracers in oceanography, paleoceanography, and ice sheet dynamics. In: Elderfield, H. (Ed.), Treatise on Geochemistry. Elsevier, New York, pp. 453–489.

Grasse, P., Stichel, T., Stumpf, R., Stramma, L., Frank, M., 2012. The distribution of neodymium isotopes and concentrations in the Eastern Equatorial Pacific: water mass advection versus particle exchange. Earth Planet. Sci. Lett. 353–354, 198–207.

Henderson, G.M., Anderson, R.F., Adkins, J., Andersson, P., Boyle, E.A., Cutter, G., de Baar, H., Eisenhauer, A., Frank, M., Francois, R., Orians, K., Gamo, T., German, C., Jenkins, W., Moffett, J., Jeandel, C., Jickells, T., Krishnaswami, S., Mackey, D., Measures, C.I., Moore, J.K., Oschlies, A., Pollard, R., Rutgers van der Loeff, M.M., Schlitzer, R., Sharma, M., von Damm, K., Zhang, J., 2007. GEOTRACES – an international study of the global marine biogeochemical cycles of trace elements and their isotopes. Chem. Erde 67, 85–131.

Jacobs, S.S., Amos, A.F., Bruchhausen, P.M., 1970. Ross sea oceanography and antarctic bottom water formation. Deep-Sea Res. Oceanogr. Abstr. 17, 935–962.

Jacobsen, S.B., Wasserburg, G.J., 1980. Sm–Nd isotopic evolution of chondrites. Earth Planet. Sci. Lett. 50, 139–155.

Jeandel, C., 1993. Concentration and isotopic compositions of Nd in the South Atlantic Ocean. Earth Planet. Sci. Lett. 117, 581–591.

Jeandel, C., Thouron, D., Fieux, M., 1998. Concentrations and isotopic compositions of neodymium in the eastern Indian Ocean and Indonesian straits. Geochim. Cosmochim. Acta 62, 2597–2607.

Jeandel, C., Arsouze, T., Lacan, F., Techine, P., Dutay, J., 2007. Isotopic Nd compositions and concentrations of the lithogenic inputs into the ocean: a compilation, with an emphasis on the margins. Chem. Geol. 239, 156–164.

Kawabe, M., Fujio, S., 2010. Pacific ocean circulation based on observation. J. Oceanogr. 66, 389–403.

Lacan, F., Jeandel, C., 2001. Tracing Papua New Guinea imprint on the central Equatorial Pacific Ocean using neodymium isotopic compositions and Rare Earth Element patterns. Earth Planet. Sci. Lett. 186, 497–512.

Lacan, F., Jeandel, C., 2004. Neodymium isotopic composition and rare earth element concentrations in the deep and intermediate Nordic Seas: constraints on the Iceland Scotland Overflow Water signature. Geochem. Geophys. Geosyst. 5, Q11006.

Lacan, F., Jeandel, C., 2005. Acquisition of the neodymium isotopic composition of the North Atlantic Deep Water. Geochem. Geophys. Geosyst. 6, Q12008.

Lang-Farmer, G., Licht, K., Swope, R.J., Andrews, J., 2006. Isotopic constraints on the provenance of fine-grained sediment in LGM tills from the Ross Embayment, Antarctica. Earth. Planet. Sci. Lett. 249, 90–107.

Molina-Kescher, M., Frank, M., Hathorne, E., 2014. South Pacific dissolved Nd isotope compositions and rare earth element distributions: water mass mixing versus biogeochemical cycling. Geochim. Cosmochim. Acta 127, 171–189.

Nowlin, W.D., Whitworth, T., Pillsbury, R.D., 1977. Structure and transport of the Antarctic Circumpolar Current at Drake Passage from short-term measurements. J. Phys. Oceanogr. 7, 778–802.

Orsi, A.H., Wiederwohl, C.L., 2009. A recount of Ross Sea waters. Deep-Sea Res., Part 2, Top. Stud. Oceanogr. 56, 778–795.

Orsi, A.H., Whitworth III, T., Nowlin Jr, W.D., 1995. On the meridional extent and fronts of the Antarctic Circumpolar Current. Deep-Sea Res., Part 1, Oceanogr. Res. Pap. 42, 641–673.

Orsi, A.H., Johnson, G.C., Bullister, J.L., 1999. Circulation, mixing, and production of Antarctic Bottom Water. Prog. Oceanogr. 43, 55–109.
Pahnke, K., van de Flierdt, T., Jones, K.M., Lambelet, M., Hemming, S.R., Goldstein, S.L., 2012. GEOTRACES intercalibration of neodymium isotopes and rare earth element concentrations in seawater and suspended particles. Part 2: systematic tests and baseline profiles. Limnol. Oceanogr., Methods 10, 252–269.
Pearce, C.R., Jones, M.T., Oelkers, E.H., Pradoux, C., Jeandel, C., 2013. The effect of particulate dissolution on the neodymium (Nd) isotope and Rare Earth Element (REE) composition of seawater. Earth. Planet. Sci. Lett. 369, 138–147.
Piepgras, D.J., Jacobsen, S.B., 1988. The isotopic composition of neodymium in the North Pacific. Geochim. Cosmochim. Acta 52, 1373–1381.
Piepgras, D.J., Wasserburg, G.J., 1987. Rare earth element transport in the western North Atlantic inferred from Nd isotopic observations. Geochim. Cosmochim. Acta 51, 1257–1271.
Reid, J.L., 1994. On the total geostrophic circulation of the North Atlantic Ocean: flow patterns, tracers, and transports. Prog. Oceanogr. 33, 1–92.
Reid, J.L., Lynn, R.J., 1971. On the influence of the Norwegian–Greenland and Weddell seas upon the bottom waters of the Indian and Pacific oceans. Deep-Sea Res. 18, 1063–1088.
Rempfer, J., Stocker, T.F., Joos, F., Dutay, J.C., Siddall, M., 2011. Modelling Nd-isotopes with a coarse resolution ocean circulation model: sensitivities to model parameters and source/sink distributions. Geochim. Cosmochim. Acta 75, 5927–5950.
Rickli, J., Frank, M., Halliday, A.N., 2009. The hafnium–neodymium isotopic composition of Atlantic seawater. Earth Planet. Sci. Lett. 280, 118–127.
Rickli, J., Frank, M., Baker, A.R., Aciego, S., de Souza, G., Georg, R.B., Halliday, A.N., 2010. Hafnium and neodymium isotopes in surface waters of the eastern Atlantic Ocean: implications for sources and inputs of trace metals to the ocean. Geochim. Cosmochim. Acta 74, 540–557.
Rickli, J., Gutjahr, M., Vance, D., Fischer Gödde, M., Hillenbrand, C.D., Kuhn, G., 2014. Neodymium and hafnium boundary contributions to seawater along the West Antarctic continental margin. Earth Planet. Sci. Lett. 394, 99–110.
Roy, M., van de Flierdt, T., Hemming, S.R., Goldstein, S.L., 2007. $^{40}Ar/^{39}Ar$ ages of hornblende grains and bulk Sm/Nd isotopes of circum-Antarctic glacio-marine sediments: implications for sediment provenance in the southern ocean. Chem. Geol. 244, 507–519.
Siddall, M., Khatiwala, S., van de Flierdt, T., Jones, K., Goldstein, S.L., Hemming, S., Anderson, R.F., 2008. Towards explaining the Nd paradox using reversible scavenging in an ocean general circulation model. Earth Planet. Sci. Lett. 274, 448–461.
Sigmon, D.E., Nelson, D.M., Brzezinski, M.A., 2002. The Si cycle in the Pacific sector of the Southern Ocean: seasonal diatom production in the surface layer and export to the deep sea. Deep-Sea Res., Part 2, Top. Stud. Oceanogr. 49, 1747–1763.
Stichel, T., Frank, M., Rickli, J., Haley, B.A., 2012. The hafnium and neodymium isotope composition of seawater in the Atlantic sector of the Southern Ocean. Earth Planet. Sci. Lett. 317, 282–294.
Stichel, T., Hartman, A.E., Duggan, B., Goldstein, S.L., Scher, H., Pahnke, K., 2015. Separating biogeochemical cycling of neodymium from water mass mixing in the Eastern North Atlantic. Earth Planet. Sci. Lett. 412, 245–260.
Tachikawa, K., Athias, V., Jeandel, C., 2003. Neodymium budget in the modern ocean and paleo-oceanographic implications. J. Geophys. Res. 108, 3254.
Talley, L.D., 1996. Antarctic intermediate water in the South Atlantic. In: Wefer, G., Berger, W.H., Siedler, G., Webb, D. (Eds.), The South Atlantic: Present and Past Circulation. Springer-Verlag, pp. 219–238.
Talley, L.T., Pickard, G.L., Emery, W.J., Swift, J.H., 2011. Descriptive Physical Oceanography: An Introduction, 6th ed. Academic Press.
Tsuchiya, M., Talley, L.D., 1996. Water-property distributions along an eastern Pacific hydrographic section at 135 W. J. Mar. Res. 54, 541–563.
van de Flierdt, T., Hemming, S.R., Goldstein, S.L., Abouchami, W., 2006. Radiogenic isotope fingerprint of Wilkes Land–Adélie Coast Bottom Water in the circum-Antarctic Ocean. Geophys. Res. Lett. 33, L12606.
van de Flierdt, T., et al., 2012. GEOTRACES intercalibration of neodymium isotopes and rare earth element concentrations in seawater and suspended particles. Part 1: reproducibility of results for the international intercomparison. Limnol. Oceanogr., Methods 10, 234–251.
Whitworth, T., Nowlin, W.D., 1987. Water masses and currents of the Southern Ocean at the Greenwich Meridian. J. Geophys. Res. 92, 6462–6476.
Whitworth, T., Orsi, A.H., Kim, S.-J., Nowlin, W.D., 1998. Water masses and mixing near the antarctic slope front. In: Ocean, Ice and Atmosphere: Interactions at the Antarctic Continental Margin, vol. 75, pp. 1–27.